J Ind Microbiol Biotechnol
DOI 10.1007/s10295-015-1694-6

Biosynthesis of mercapturic acid derivative of the labdane-type diterpene, cyslabdan that potentiates imipenem activity against methicillin-resistant *Staphylococcus aureus*: cyslabdan is generated by mycothiol-mediated xenobiotic detoxification

Haruo Ikeda[1] · Kazuo Shin-ya[2] · Tohru Nagamitsu[3] · Hiroshi Tomoda[3]

Received: 16 July 2015 / Accepted: 21 September 2015

Abstract Genome mining of cyslabdan-producing *Streptomyces cyslabdanicus* K04-0144 revealed that a set of four genes, *cldA*, *cldB*, *cldC*, and *cldD* (the *cld* cluster), which formed a single transcriptional unit, were involved in the biosynthesis of cyslabdan that potentiates imipenem activity against methicillin-resistant *Staphylococcus aureus*. Experimental studies supported the heterologous expression of the *cld* cluster of *S. cyslabdanicus* K04-0144 in *S. avermitilis* SUKA22, and transformants carrying the *cld* cluster produced not only cyslabdan A (**1**), but also its new derivatives, 17-hydroxyl-**1** (**2**) and 2-hydroxyl-**1** (**3**), in the culture broth. An analysis of diterpene metabolites in the mycelia showed that a large amount of a novel intermediate had accumulated and its structure was elucidated as (*7S, 8S, 12E*)-8,17-epoxy-7-hydroxylabda-12,14-diene (**4**). The *cld*-like cluster (*rmn* cluster) was also detected in the genome of *S. anulatus* GM95 by searching our in-house genome databases, and the heterologous expression of the *rmn* cluster in *S. avermitilis* SUAK22 demonstrated that the *rmn* cluster was involved in the biosynthesis of the labdane-type bicyclic diterpene, raimonol (**7**). CldA/RmnA catalyzed the generation of geranylgeranyl diphosphate (GGPP) from dimethylallyl diphosphate and isopentenyl diphosphate. CldB/RmnB converted GGPP to (+)-copalyl diphosphate, and CldD/RmnD generated labda-8(17),12(*E*),14-triene (**5**). CldC introduced two oxygen atoms at C-7 and C-8,17 to generate **4**, while RmnC hydroxylated **5** at C-7 to generate **7**. The heterologous expression of the *cld* cluster suggested that four gene products catalyzed to generate **4**, but not **1**. The deletion mutant of the gene encoding the mycothiol (MSH)-*S*-conjugate amidase (*mca*) of *S. avermitilis* SUKA22 carrying the *cld* cluster failed to produce **1**, but accumulated **4** in the mycelia, whereas *S. avermitilis* SUKA22 and its *mca*-deletion mutant carrying the *cld* cluster both produced the MSH-*S*-conjugate of **4**. The intermediate **4** was converted into the MSH-*S*-conjugate with MSH, which was achieved through a non-enzymatic nucleophilic reaction. The MSH-*S*-conjugate of **4** generated was further hydrolyzed to generate the mercapturic acid derivative, **1**, by MSH-*S*-conjugate amidase and **1** was excreted from the mycelia.

Keywords Genome mining · Biosynthesis · Labdane-type diterpene · Heterologous expression · Mycothiol

Special Issue: Natural Product Discovery and Development in the Genomic Era. Dedicated to Professor Satoshi Ōmura for his numerous contributions to the field of natural products and congratulated him on the winning of The Nobel Prize in Physiology or Medicine 2015.

Electronic supplementary material The online version of this article (doi:10.1007/s10295-015-1694-6) contains supplementary material, which is available to authorized users.

✉ Haruo Ikeda
ikeda@ls.kitasato-u.ac.jp

[1] Kitasato Institute for Life Sciences, Kitasato University, 1-15-1 Kitasato, Sagamihara, Kanagawa 252-0373, Japan

[2] National Institute of Advanced Industrial Science and Technology, 2-4-7 Aomi, Koto-ku, Tokyo 135-0064, Japan

[3] School of Pharmacy, Kitasato University, 5-9-1 Shirokane, Minato-ku, Tokyo 108-8641, Japan

Introduction

Methicillin-resistant *Staphylococcus aureus* (MRSA) is one of the major nosocomial pathogens that have developed resistance to many antibiotics. Therefore, new antimicrobial agents and measures that are effective against MRSA infections need to be developed. During a screening

Published online: 27 October 2015

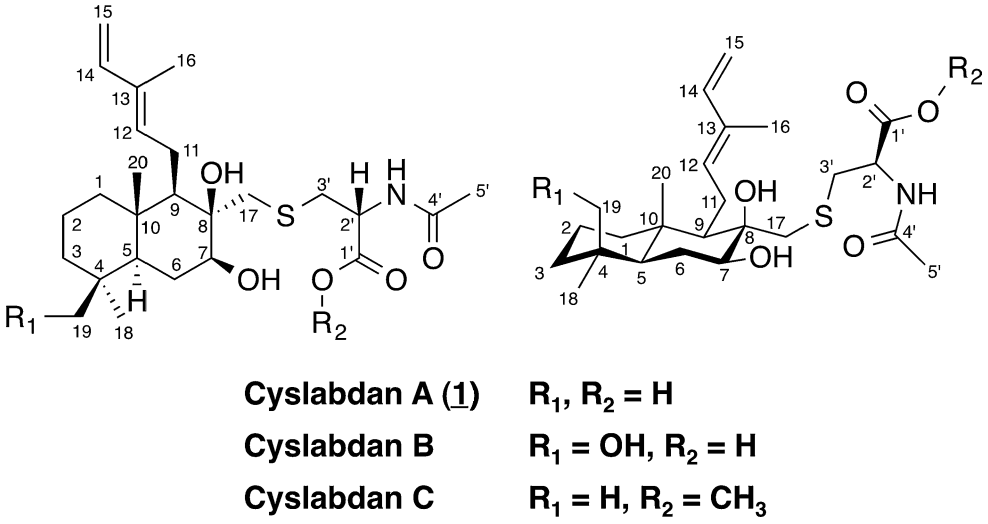

Fig. 1 Structures of cyslabdans A, B, and C produced by *S. cyslabdanicus* K04-0144

program, mercapturic acid derivatives of a non-antibiotic diterpene, cyslabdans A (**1**), B, and C (Fig. 1), were identified as potentiators of the β-lactam antibiotic, imipenem, which exhibits activity against MRSA [11, 24]. **1** was found to be the most effective component. The structures of cyslabdans have recently been revised in studies on the total synthesis of **1** [31]. **1** was previously reported to enhance the activity of β-lactam antibiotics against MRSA by 8–32-fold (penam), 4–32-fold (cephem), and 128 to over 1000-fold (carbapenem); however, the compound itself did not exhibit antimicrobial activity. The activities of other typical antibiotics, such as streptomycin, vancomycin, tetracycline, and ciprofloxacin, were not enhanced by **1** [12]. A previous study on the mechanism of action of **1** revealed that the compound specifically bound to the FemA of MRSA, which is involved in the pentaglycine interpeptide bridge of the peptidoglycan of MRSA, and monoglycyl or nonglycyl murein monomers accumulated in MRSA. However, **1** itself had almost no effect on the growth of MRSA, indicating that the penicillin-binding protein (PBP) and/or PBP2′ recognized monoglycyl murein monomers as a substrate and cross-linked them to construct peptidoglycans. A treatment with a combination of imipenem and cyslabdan was shown to completely inhibit the growth of MRSA, indicating that imipenem-insensitive PBP2′ was not able to cross-link monoglycyl murein monomers, resulting in the failed formation of MRSA peptidoglycans [25].

Although many terpene metabolites have been isolated from fungi and plants, only a relatively minor fraction of these widely occurring metabolites has been identified in bacteria including *Streptomyces* microorganisms. The major terpene metabolites of *Actinomycetales* microorganisms are the degraded sesquiterpene alcohol, geosmin, and monoterpene alcohol, 2-methylisoborneol, and some diterpene metabolites (such as hydrocarbon or alcohol) have also been isolated from *Actinomycetales* microorganisms [39]. **1** produced by *Streptomyces cyslabdanicus* K04-0144 has a unique labdane-type bicyclic diterpene backbone that is connected to *N*-acetylcysteine via a thioester linkage (mercapturic acid derivative). Diterpene metabolites including hydrocarbons, alcohol, and oxidized derivatives have been detected in fungal and plant metabolites; however, the mercapturic acid derivatives of terpene have rarely been detected in bacterial, fungal, or plant metabolites.

In the present study, we cloned genes involving the formation of the **1** backbone and also revealed that the low-molecular-weight thiol compound, mycothiol, was involved in the formation of **1**.

Materials and methods

Bacterial strains and plasmid vectors

Streptomyces cyslabdanicus K04-0144 and *S. anulatus* GM95 were used to isolate genomic DNA. *S. avermitilis* SUKA22 [23] was used as a host for the heterologous expression of the biosynthetic gene cluster and in the construction of *mca*-deletion mutants. The bacterial growth conditions for the isolation of terpene metabolites have been described previously [40]. The integrating vector pKU460 [22] was used to clone the *cld* or *rmn* biosynthetic gene clusters and express the gene encoding cytochrome P450 (*cldC*). pKU257 [22], for which replication in *S. avermitilis* was unstable, was used for the gene disruption of the *S. avermitilis* genome by allelic replacement. Cloning, transformation, conjugation, and the *E. coli* strains used were described previously [15, 21, 22]. The mutant *loxP* sequence (*mut-loxP*) [1] was used for the deletion cassettes.

Cloning of the *cld* cluster

The chromosomal DNA of *S. cyslabdanicus* K04-0144 was sheared by repeated passing through a 23-gauge needle (500 times) to generate fragments of approximately 40 kb. After purification by agarose gel electrophoresis, the 40-kb fragments were treated with *Bal*31 at 25 °C for 15 s and both ends of the fragments were filled by a DNA Blunting kit (Takara Bio Inc. Japan). The blunt-ended DNA fragments were ligated with the large *Swa*I segment of pKU402 [16] and ligated DNA was then subjected to in vitro packaging. Positive clones were selected by colony PCR of each cosmid clone using two pairs of primers: forward for PF00348: 5′-GTTCCAGACCTTCGCCCTGATCC-3′ and reverse for PF00348: 5′-CACCGAAGACGTTGAGCAG GTCAT-3′, and forward for PF03936: 5′-ATCTGGT GCTGTTCGCGGAACTC-3′ and reverse for PF03936: 5′-CGTAGGAGGCCAAGTCGTTGATCC-3′. After a cosmid clone (from twelve positive clones) containing the entire *cld* cluster was digested with *Mfe*I and *Bsp*LU11I and the digest was separated by agarose gel electrophoresis, the largest 12.4-kb *Mfe*I/*Bsp*LU11I fragment was purified from the agarose gel. A 12.4-kb *Mfe*I/*Bsp*LU11I fragment was ligated with the large *Mfe*I/*Bsp*LU11I fragment of the integrating vector pKU460 to generate pCLD101. The region of the strong constitutive promoter P_{rpsJ} was amplified from pKU1021 [22] by PCR using the primer pair, forward: 5′-CGAACGGATATAAGGGTCGGGATATCG GTGTCCCATGCGGTACCGGC**catATGTACTCAG TAGTCCTTCGTCTCGAT**-3′ (underlined and bold characters correspond to the N-terminal region of *cldA* and region of the *rpsJ* promoter of *S. avermitilis*, respectively, while lowercase characters indicate the start codon of *cldA*) and reverse: 5′-GGGTAACGCCAGGGTTTTCC CAGTCACGACGTTGTAAAACGACGGCCAGT**AGC GATCTCGGCTTGAACGAATTG**-3′ (underlined and bold characters correspond to the regions of pCLD101 and *aac(3)I* of pKU1021, respectively). The amplified segment was treated with *Dpn*I to remove template DNA and used to introduce the *rpsJ* promoter upstream of the *cld* biosynthetic gene cluster. Initial denaturation (96 °C for 180 s) was followed by 5 cycles of amplification (95 °C for 30 s, 50 °C for 30 s, and 72 °C for 90 s) and 25 cycles (95 °C for 30 s, 68 °C for 90 s), and then a final incubation at 72 °C for 5 min using Phusion DNA polymerase (New England Biolabs, MA, USA). The amplified segment was treated with *Dpn*I to remove template DNA. The amplicon containing the *rpsJ* promoter and resistance marker, *aac(3)I,* was co-transformed into L-arabinose-induced *E. coli* BW25141 carrying pKD46 [9] with *Nru*I-cut pCLD101. The desired plasmids (expression of the biosynthetic gene cluster was controlled by the *rpsJ* promoter) were obtained by selection with 50 μg/ml kanamycin and 25 μg/ml fortimicin (*aac(3)I*) and confirmed by restriction digestion to obtain pCLD102.

To construct the in-frame deletion of *cldC* in pCLD102, *loxP-aadA-loxP* of pKU478 [22] was amplified by PCR using the primer pair: forward: 5′-CCGTTCCGCCGC CCCTTCAGCCCGGACCGCATTCGGAGGAACCAC CTGTGT**CAGTGAGTTCGAGCGACTCGAGT**-3′ (underlined and bold characters correspond to the upstream region of *cldC* and the region of *loxP-aadA-loxP*, respectively) and reverse: 5′-AGGCAGAATCGTCACCG CATCGCCGGTGCGGGTCATGCGGCCTCCTGGTG G**CTGGTACCGAGCGAACGCGTT**-3′ (underlined and bold characters correspond to the downstream region of *cldC* and the region of *loxP-aadA-loxP*, respectively). Initial denaturation at 96 °C for 180 s was followed by 5 cycles of amplification (95 °C for 30 s, 50 °C for 30 s, and 72 °C for 90 s), 25 cycles (95 °C for 30 s and 68 °C for 90 s), and then a final incubation at 72 °C for 5 min. After amplification, the reaction mixture was treated with *Dpn*I to remove template DNA. The 1.27-kb amplicon of the resistance marker segment carrying the upstream and downstream sequences of the *cldC* gene cluster was co-transformed into L-arabinose-induced *E. coli* BW25141 carrying pKD46 with *Bsu*36I-cut pCLD102 by electroporation. The desired plasmid, pCLD102*ΔcldC::loxP-aadA-loxP*, was obtained by selection with 50 μg/ml kanamycin, 50 μg/ml of streptomycin (*aadA*) and 100 μg/ml of spectinomycin (*aadA*), and was confirmed by restriction digestion. To remove the marker gene, *aadA*, pCLD102*ΔcldC::loxP-aadA-loxP* was treated with Cre recombinase (New England Biolabs, USA). The reaction mixture was then treated with *Swa*I to remove the unreacted product. Since two *Swa*I sites were located inside the *aadA* region, unreacted pCLD102*ΔcldC::loxP-aadA-loxP* was linearized whereas the desired plasmid, pCLD102*ΔcldC*, was not. The *Swa*I-treated preparation was introduced into *E. coli* DH5α and the desired clones were selected by kanamycin-resistance and streptomycin/spectinomycin-sensitive phenotypes. pCLD104 (pCLD102*ΔcldC*) was obtained by the confirmation of restriction digestion.

Cloning of the *rmn* cluster

To clone the entire *rmn* gene cluster from *S. anulatus* GM95, the chromosomal DNA of *S. anulatus* GM95 was completely digested with *Bam*HI and *Pst*I. Neither restriction sites were located inside of the entire gene cluster. Eight-kilobase fragments were purified by agarose gel electrophoresis. A linearized cloning vector was prepared by PCR amplification with pRED [22] as template DNA using a designated primer pair, both of which contained 50-nt sequences corresponding to the upstream and downstream regions of the *rmn* gene cluster, forward:

5′-GCCGTACGGACGGGAGGTCCGGCAGACTCGTG GTGGGACAGGTTTTTGC*cat*ATG**TGCCAGGAA GATACTTAACAG**-3′ (underlined, italicized, and bold characters correspond to the upstream region of the *rmn* cluster, the *Nde*I site, and the region of the vector pRED, respectively, and lowercase characters indicate the start codon of *rnmA*) and reverse: 5′-GAACCCGGTCGAGCT GCCGCTGGGCGCGCCGCCGCGCGTGCTGAACCTC G*AAGCTT***CCATTCATCCGCTTATTATC**-3′ (underlined, italicized, and bold characters indicate the downstream region of the *rmn* cluster, the *Hin*dIII site, and the region of the vector pRED, respectively). Initial denaturation at 96 °C for 180 s was followed by 5 cycles of amplification (95 °C for 30 s, 50 °C for 30 s, and 72 °C for 100 s), 25 cycles (95 °C for 30 s and 68 °C for 100 s), and then a final incubation at 72 °C for 5 min. After amplification, the reaction mixture was treated with *Dpn*I to remove template DNA. The 1.7-kb amplicon of pRED carrying the upstream and downstream sequences of the *rmn* gene cluster was co-transformed into L-arabinose-induced *E. coli* BW25141 carrying pKD46 with the size-fractionated chromosomal DNA of *Bam*HI/*Pst*I-cut *S. anulatus* GM95 by electroporation. The desired plasmid, pRED carrying the entire *rmn* cluster, was obtained by selection with 30 μg/mL chloramphenicol and was also confirmed by restriction digestion. The large *Nde*I/*Hin*dIII fragment of pRED carrying the entire *rmn* cluster was ligated with the large fragment of *Nde*I/*Hin*dIII-pKU1021 to generate pRMN102.

Construction of a cassette for the expression of *cldC*

A gene encoding cytochrome P450 (*cldC*) was amplified by PCR with pCLD101 as a template DNA using the primer pair: forward 5′-AGGGCGAGCAT**atgAACAC CGACCTGCACTTTCCGCC**-3′ (underlined and bold characters correspond to the *Nde*I site and N-terminal region of *cldC,* respectively, and lowercase characters indicate the start codon of *cldC*) and reverse: 5′-TTCGA GAAGCTTG**tcaTGCGGCCTCCTGGTGGCGGC**-3′ (underlined and bold characters correspond to the *Hin*dIII site and C-terminal region of *cldC,* respectively, and lowercase characters indicate the stop codon of *cldC*). Initial denaturation at 96 °C for 180 s was followed by 25 cycles of amplification (95 °C for 30 s, 60 °C for 30 s, and 72 °C for 90 s) and then a final incubation at 72 °C for 5 min. After amplification, the reaction mixture was treated with *Dpn*I to remove template DNA. The amplified DNA was digested with *Nde*I and *Hin*dIII, and the *Nde*I/*Hin*dIII amplicon then was ligated with the large *Nde*I/*Hin*dIII-pKU1021 (the integrating vector contained the *rpsJ* promoter) to generate pKU1021*::cldC*.

Construction of *mca*-deletion mutants

To construct deletions of *mca* (*sav3299*) in *S. avermitilis*, two segments were prepared by PCR amplification with template DNA from the *S. avermitilis* cosmid CL_238_G10 [17] (http://avermitilis.ls.kitasato-u.ac.jp/cosmid/) using the primer pair of the upstream region: forward: 5′-GAATG GAAGCTTGCCTGCTGCGCGGCGACCTGTACC-3′ (underlined characters indicate the *Hin*dIII site) and reverse: 5′-TACCAGTGTACACTGACCCCGCCGAGCCGACA GCAC-3′ (underlined characters indicate the *Bsr*GI site), and the primer pair of the downstream region: forward: 5′-TCACTGTGTACATCAAGGCTCAATCCTCAGTAA GTCGG-3′ (underlined characters indicate the *Bsr*GI site) and reverse: 5′-CTGGCAGAATTCGCGGGCTACACGGT CATCGACT-3′ (underlined characters indicate the *Eco*RI site), respectively. The cloning vector pRED and resistance marker *loxP-aphII-loxP* were also amplified by PCR using the primer pair of the pRED vector, forward: 5′-CTCGAGA AGCTTCCATTCATCCGCTTATTATC-3′ (underlined characters indicate the *Hin*dIII site) and reverse: 5′-CTCGAG GAATTCTGCCAGGAAGATACTTAACAG-3′ (underlined characters indicate the *Eco*RI site), and the primer pair for the resistance marker: forward: 5′-CTCGAGTGTA CACTTCATGAGCTCAGCCAATC-3′ (underlined characters indicate the *Bsr*GI site) and reverse: 5′-CTCGAGT GTACATGCCGTATTTGCAGTACCAG-3′ (underlined characters indicate the *Bsr*GI site), respectively. Initial denaturation at 96 °C for 180 s was followed by 25 cycles of amplification (95 °C for 30 s, 60 °C for 30 s, and 72 °C for 90 s) and then a final incubation at 72 °C for 5 min. After amplification of the above segments, the upstream segment digested with *Hin*dIII and *Bsr*GI, the downstream segment digested with *Bsr*GI and *Eco*RI, the vector segment digested with *Eco*RI and *Hin*dIII, and the resistance marker segment digested with *Bsr*GI were ligated together in a molar ratio of 1:1:1:1. *E. coli* DH5α was transformed with the ligated products, the transformants were selected by chloramphenicol (30 μg/ml) and kanamycin (50 μg/ml), and the desired clones were confirmed by restriction digestion. The vector region of the disruption cassette was replaced by pKU257 using the homologous regions *cat* and p15A in both vectors using the RecE/RecT-mediated recombination system of *E. coli* JC8679 (*recBC sbcA*) *Δ(srl-recA)*::Tn*10*. The pKU257 plasmid carrying the disruption cassette was introduced into SUKA22 by conjugation, and the desired disruptants obtained by allelic replacement were selected using thiostrepton-sensitive and neomycin-resistance markers. The deletion region was confirmed by PCR amplification and Southern hybridization, and the resistance marker in the disruptant was then removed by introducing the *cre*-expression vector pKU471 [22].

Detection of diterpene metabolites

The spores of all *Streptomyces* strains including transformants of engineered *S. avermitilis* were grown in vegetative medium [6] at 30 °C for 2 days on a reciprocal shaker (200 strokes per min). A 0.15-ml portion of the vegetative culture was inoculated into 15 ml of the production medium [6] in a 125-ml flask. *S. cyslabdanicus* K04-0144 was further examined in the complex production medium described previously [11]. After incubation at 28 °C for 5 days on the rotary shaker at 200 rpm, the whole culture was centrifuged at 3000 rpm for 10 min. Sedimented mycelia were extracted with 5 ml of methanol and removed by centrifugation. Each culture supernatant and methanol extract of mycelia were analyzed by high-performance liquid chromatography (HPLC) (ELITE LaChrom system, Hitachi Co. Japan) connected with quadrupole time-of-flight mass spectrometry (Q-TofMS) (Micromass, Q-Tof Ultra™ API), HPLC/TofMS (Acquity ultraperformance LC system, Waters Xevo G2-S Tof), or GC–MS (Shimadzu GC-17A; 70 eV, electron ionization, positive ion mode; 30 m × 0.25 mm InterCap 5 capillary column [diphenyl (5 %)-dimethyl (95 %) polysiloxane; GL Sciences] using a temperature program of ~50–280 °C and temperature gradient of 20 °C/min). Compounds produced were evaluated by comparison with the mass spectra of the corresponding reference compounds in the GC–MS databases, NIST/EPA/NIH MS Library (2014 version).

Isolation of diterpene metabolites by heterologous expression

Two liters of the culture growing *S. avermitilis* SUKA22 carrying pCLD102 (harboring the entire *cld* cluster of *S. cyslabdanicus* K04-0144) in the production medium [6] at 28 °C for 6 days was centrifuged at 6000 rpm for 20 min to separate mycelia and the supernatant. The clarified supernatant was applied to the synthetic resin, SP825 (10 g; Mitsubishi Chemical Co. Japan). After the resin was washed with 50 ml of deionized water, active principles were eluted with 100 ml of 80 v/v % methanol water and concentrated to remove methanol. Approximately, 100 ml of deionized water was added and **1** was removed by extraction twice with 25 ml of ethyl acetate. The aqueous layer was applied on a SP825 column (10 × 20 mm, Mitsubishi Chemical Co. Japan) and the column was washed with deionized water. The materials were eluted with 10 ml of 80 v/v % methanol. The eluate was concentrated to dryness and the material was dissolved in 1 ml of deionized water. Each component was purified by preparative HPLC (PEGASIL ODS, 20 × 250 mm; mobile phase, 60 v/v % CH_3CN in 0.05 w/v % formic acid for **2** and 30 v/v % CH_3CN in 0.05 w/v % formic acid for **3**; flow rate, 8.0 ml/min; detection, UV at 210 nm). Under these conditions, **2** was eluted as a peak with a retention time of 22.5 min and **3** as a peak with a retention time of 17.2 min. Each fraction was applied on a SP825 column to remove formic acid. After washing with deionized water, each component was eluted with methanol and concentrated to yield a white powder (**2**; 10 mg and **3**; 7 mg).

The mycelia centrifuged from above were suspended in 500 ml of water, and the suspension was re-centrifuged at 6000 rpm for 20 min. Washed mycelia were extracted twice with 500 ml of methanol and mycelia were then removed by filtration. The methanol extract was concentrated under reduced pressure to yield a brownish oily material (1.8 g). The oily material was dissolved in 50 ml of *n*-hexane and insoluble materials were removed by filtration. The *n*-hexane extract was dried over anhydrous Na_2SO_4 and concentrated to approximately 5 ml under reduced pressure. The concentrate was subjected to silica gel column chromatography (20 × 200 mm). The column was washed with *n*-hexane to remove undesired materials and the active material was eluted by *n*-hexane/ethyl acetate (10:1). **4** was purified by preparative HPLC (PEGASIL ODS, 20 × 250 mm; mobile phase, 70 v/v % CH_3CN in 0.05 w/v % formic acid; flow rate, 8.0 ml/min; detection, UV at 210 nm) as an amorphous powder (12 mg).

The bicyclic diterpene hydrocarbon **5** was prepared from *S. avermitilis* SUKA22 carrying pCLD104. Two liters of the culture grown in the production medium was centrifuged at 6000 rpm for 20 min to remove the supernatant. The sedimented mycelia were suspended in 250 ml of water and the suspension was then centrifuged. Washed mycelia were extracted twice with 500 ml of methanol, the mycelia were removed by filtration, and the methanol extract was re-extracted twice with 200 ml of *n*-hexane. The *n*-hexane extract was washed with 100 ml of 0.1 N NaOH to remove free fatty acids. The organic phase was dried over anhydrous Na_2SO_4 and evaporated to dryness (brownish oily material; 1.0 g). The residual brownish syrup was dissolved in a small volume of *n*-hexane and subjected to silica gel column chromatography (15 × 150 mm) developed with *n*-hexane. Each fraction (2 ml) was analyzed by GC–MS and fractions containing the diterpene hydrocarbon **5** were pooled and concentrated to obtain 20 mg of **5** as transparent oil.

The diterpene metabolites **7** and **8**, which were detected in the heterologous expression of the *rmn* cluster of *S. anulatus* GM95, were prepared from *S. avermitilis* SUKA22 carrying pRMN102. Two liters of the culture grown in the production medium was centrifuged at 6000 rpm for 20 min. The sedimented mycelia were washed with 500 ml of water and harvested by centrifugation. After washed mycelia had been extracted twice with 500 ml of methanol, they were removed by filtration. The methanol extract

was evaporated to remove methanol under reduced pressure. After the concentrate was diluted with 100 ml water, the mixture was extracted twice with 50 ml of ethyl acetate. The organic layer was dried over anhydrous Na_2SO_4 and evaporated under the reduced pressure to yield brownish oily material (ca. 1.0 g). The residual brownish syrup was dissolved in a small volume of *n*-hexane and subjected to silica gel column chromatography (20 × 100 mm) developing with *n*-hexane. After the column was washed with *n*-hexane, **7** and **8** were eluted with CH_2Cl_2 and CH_2Cl_2/methanol (20:1), respectively. Fraction containing **7** was applied to silica gel chromatography (10 × 50 mm) developing with CH_2Cl_2 as a white amorphous powder (12 mg). The fraction containing **8** was purified by preparative HPLC (PEGASIL ODS, 20 × 250 mm; mobile phase, 50 v/v % CH_3CN in 0.05 w/v % formic acid; flow rate, 8.0 ml/min; detection, UV at 210 nm) as amorphous powder (7 mg).

Physicochemical analysis

1D and 2D nuclear magnetic resonance (NMR) (^{1}H: 500 MHz; ^{13}C: 125 MHz, in $CDCl_3$) spectra were both obtained on a JEOL JNM-ECP 500 FT NMR system. Abbreviations in ^{1}H NMR signals were as follows: singlet (s), multiplet (m), doublet (d), triplet (t), double doublet (dd), double triplet (dt), and broad singlet (brs) signals. High-resolution mass spectra (HR-MS) by the electrospray ionization (ESI) mode were obtained on a JEOL JMS-700 Mstation.

Results

Genome mining of the gene cluster for cyslabdan biosynthesis

We previously developed a powerful search method based on the use of hidden Markov models (HMM) and a Pfam search that has allowed the discovery of novel bacterial terpene synthases [40, 41]. Three out of a total of 7453 deduced proteins of *S. cyslabdanicus* K04-0144 were selected as possible terpene synthases with E value ranges from 6×10^{-45} to 1.2×10^{-194}. Two of these proteins were predicted to be the sesquiterpene synthases, geosmin/germacredienol synthase and *epi*-isozizaene synthase, respectively, by a phylogenetic analysis of the deduced proteins with the known terpene synthases of *Streptomyces* microorganisms [39]. Cyclic terpene metabolites were previously shown to be generated by acyclic variations of a universal cyclization mechanism that is initiated by the enzyme-catalyzed ionization of the universal acyclic precursors geranyl diphosphate (GPP), farnesyl diphosphate (FPP), and geranylgeranyl diphosphate (GGPP) to form the corresponding allylic cations [39]. In some cases, a gene cluster for cyclic terpene metabolite biosynthesis in an *Actinomycetales* microorganism contained a gene encoding the formation of prenyl diphosphate (FPP or GGPP), which is the direct precursor for terpene synthesis, located in the gene cluster (gene cluster for the pentalenolactone family metabolite [38], terpentecin [8], or viguiepinol [14]). Therefore, searching for genes encoding prenyl diphosphate synthase by a Pfam search using model PF00348 (polyprenyl synthetase) was used as a second screening for the discovery of the biosynthetic gene cluster for **1**. Five deduced proteins were selected as possible prenyl diphosphate synthases with E value ranges from 4.6×10^{-32} to 2.0×10^{-57}, and a gene encoding one of the prenyl diphosphate synthases (*cldA*) was located upstream of a gene encoding another predicted terpene synthase (*cldD*). These two genes, *cldA* and *cldD*, and an additional two genes, *cldB* and *cldC*, formed an operon (*cld* cluster: accession # LC064028) within the length of 5.5-kb region (Fig. 2).

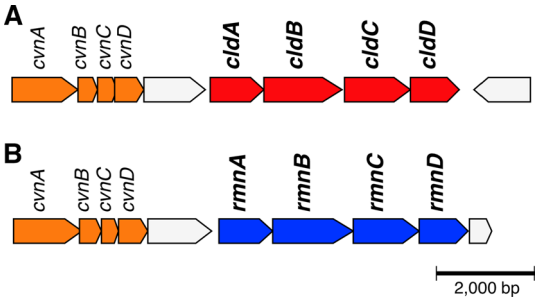

Fig. 2 Organization of genes encoding predicted biosynthesis of labdane-type diterpene metabolites and flanking genes. The biosynthetic gene clusters for cyslabdans (*cld*) filled in a *red color* and raimonol (*rmn*) filled in a *blue color* are composed of genes encoding GGPP synthase (*cldA* and *rmnA*), (+)-copalyl diphosphate synthase (*cldB* and *rmnB*), cytochrome P450 (*cldC* and *rmnC*) and labdatriene synthase (*cldD* and *rmnD*), respectively. A set of genes (filled in *orange color*) involved in the multi-component regulatory system (conservon) was located upstream of the *cld* or *rmn* cluster. Four conserved genes encoding histidine sensor kinase (*cvnA*), roadblock/LC7 domain-containing protein (*cvnB*), protein of unknown function DUF742 (*cvnC*), and ATP/GTP-binding protein (*cvnD*) were located in this region

To evaluate the biological functions of individual gene products deduced by DNA sequencing data, we searched public databases with their deduced amino acid sequences by means of an amino acid sequence similarity search by BLAST and estimation of the motif signature by Pfam. The predicted 361-aa gene product of *cldA* in the operon showed 53 % identity and 67 % positive matches to *S. clavuligerus* ATCC 27064 GGPP synthase (397-aa; ZP_06775142). The deduced prenyl diphosphate synthase, CldA, consisted of the universally conserved two divalent metal-binding motifs, acidic amino acid-rich

^{96}H**DD**VM**D** and downstream ^{242}AFQLR**DD**L [26]. The predicted 532-aa gene product of *cldB* downstream of *cldA* showed 49 % identity and 59 % positive matches to *S. clavuligerus* ATCC 27064 *ent*-copalyl diphosphate synthase (519-aa; ZP_05004574), 39 % identity and 52 % positive matches to *Streptomyces* sp. KO-3988 *ent*-copalyl diphosphate synthase (511-aa; BAD86797), which is involved in the biosynthesis of the tricyclic diterpene, viguepinol, and 33 % identity and 45 % positive matches to *Kitasatospora griseola* MF730-N6 terpentedienyl diphosphate synthase (499-aa; BAB39206), which is involved in the biosynthesis of the bicyclic diterpene, terpentecin. The first gene *cldA* was translationally coupled to the downstream gene *cldB*. Sequence alignment with eukaryotic diterpene synthases revealed that the motifs DxDDTA and QxxDGSW, which were proposed to stabilize an intermediate cation during the cyclization process and mediate substrate binding by the chelation of divalent metal ions, respectively [3, 27], were conserved in the CldB product (^{313}**DTDDTA**, ^{443}**Q**SD**DGSW**). The predicted 454-aa gene product of *cldC* downstream of *cldB* showed 42 % identity and 59 % positive matches to *Amycolatopsis mediterranei* U32 cytochrome P450 (443-aa; YP_003766987). A protein-family analysis using the Pfam database revealed that the deduced gene product CldC had a typical motif found in cytochrome P450 (PF00067) with an E value of 2×10^{-78}. The universally conserved cysteine residue found in the C-terminal region of all cytochrome P450 s and that binds the proximal face of the protoheme co-factor was found in CldC (-RQ**C**MG-) at ^{393}Cys. The last predicted 329-aa gene product of *cldD* downstream of *cldC* showed 34 % identity and 48 % positive matches to *S. clavuligerus* ATCC 27064 terpene synthase (322-aa; ZP_06775673) and 26 % identity and 43 % positive matches to *Kitasatospora griseola* MF730-N6 terpentetriene synthase (311-aa; BAB39207), which is involved in the biosynthesis of terpentecin. The gene *cldC* was translationally coupled to the downstream gene *cldD*. Since two genes, *cldB* and *cldD*, encoded the predicted (+)-copalyl diphosphate synthase and terpene synthase, their gene products, CldB and CldD, corresponded to type-B and type-A terpene synthases, respectively. The deduced type-A terpene synthase, CldD, displayed the universally conserved pair of divalent metal-binding motifs, an acidic amino acid-rich ^{90}**DD**MHG**E** and the downstream triad ^{230}**N**DYY**S**WGR**E** [34–36]. A gene predicted to be *N*-acetylmuramoyl-L-alanine amidase was located downstream of *cldD*, which was located in the opposite direction. This gene and further downstream genes may be out of the gene cluster for cyslabdan biosynthesis because the predicted functions were concerned with primary metabolism. A single transcriptional unit containing five genes was found upstream of the presumptive *cld* gene cluster. All five genes were translationally coupled with the downstream gene, and the first four genes were similar to a set of a multi-component regulatory system that is frequently found in *Streptomyces* genomes [20, 37] (Fig. 2).

Heterologous expression of the presumptive *cld* cluster

To clone the entire gene cluster for the biosynthesis of **1**, the genomic library of *S. cyslabdanicus* K04-0144 was prepared by an in vitro packing system using a cosmid vector. The desired clones were selected by colony-PCR screening of the cosmid library using two pairs of primers, which were amplified in the *cldA* and *cldD* regions, respectively, and twelve clones were positively isolated from 2304 cosmid clones. To minimize the region containing the presumptive *cld* cluster, the 12.4-kb *Mfe*I/*Bsp*LU11I fragment of a cosmid clone was subcloned into an integrating vector pKU460 (*Eco*RI/*Bsp*LU11I) and a subclone (pCLD101) was identified and confirmed by restriction cutting. *S. avermitilis* SUKA22, which is an engineered host suitable for heterologous expression, was transformed by PEG-assisted transformation using an unmethylated preparation of pCLD101. Unfortunately, *S. avermitilis* SUKA22 transformants carrying pCLD101 produced a very small amount of **1** in the culture both (Fig. 3). We previously developed the heterologous expression of many biosynthetic gene clusters using a strongly and constitutively expressed promoter in *S. avermitilis* [22]. In an attempt to improve productivity, a promoter of the gene encoding the ribosomal small protein S10 of *S. avermitilis* (*rpsJ*) was inserted in front of the first gene of the operon by λ-RED recombination, yielding pCLD102. The resulting recombinant plasmid was introduced into *S. avermitilis* SUKA22. Since **1** was produced in the culture broth in the original producer *S. cyslabdanicus* K04-0144, the transformants of *S. avermitilis* SUKA22 carrying pCLD102 were grown in production medium and the culture supernatant was directly analyzed by HPLC. The transformants produced not only **1** (*m/z* 468 $[M + H]^+$), the productivity of which was the same as the original producer *S. cyslabdanicus* K04-0144, but also abundant amounts of two new peaks, **2** and **3**, which were eluted at 7.52 and 17.05 min with parent $[M + H]^+$ *m/z* 484, respectively, in the culture broth (Fig. 3). These two components were purified from the culture broth and their structures were elucidated by several spectrum analyses. Approximately, 15 mg of **2** and 7 mg of **3** were obtained from a 2-l culture as a white powder. The molecular formula $C_{25}H_{42}NO_6S$ of **2** and **3** was obtained from HR-MS (ESI mode; observed, 484.2758: **1**, 484.2762: **2**, calcd. for 484.2727), indicating that each structure resulted from the addition of one oxygen atom to **1**. A comparative analysis of ESI–MS fragments between **1** and two compounds (**2** and **3**) indicated that these two compounds were simple hydroxylation products of **1**, respectively, based on

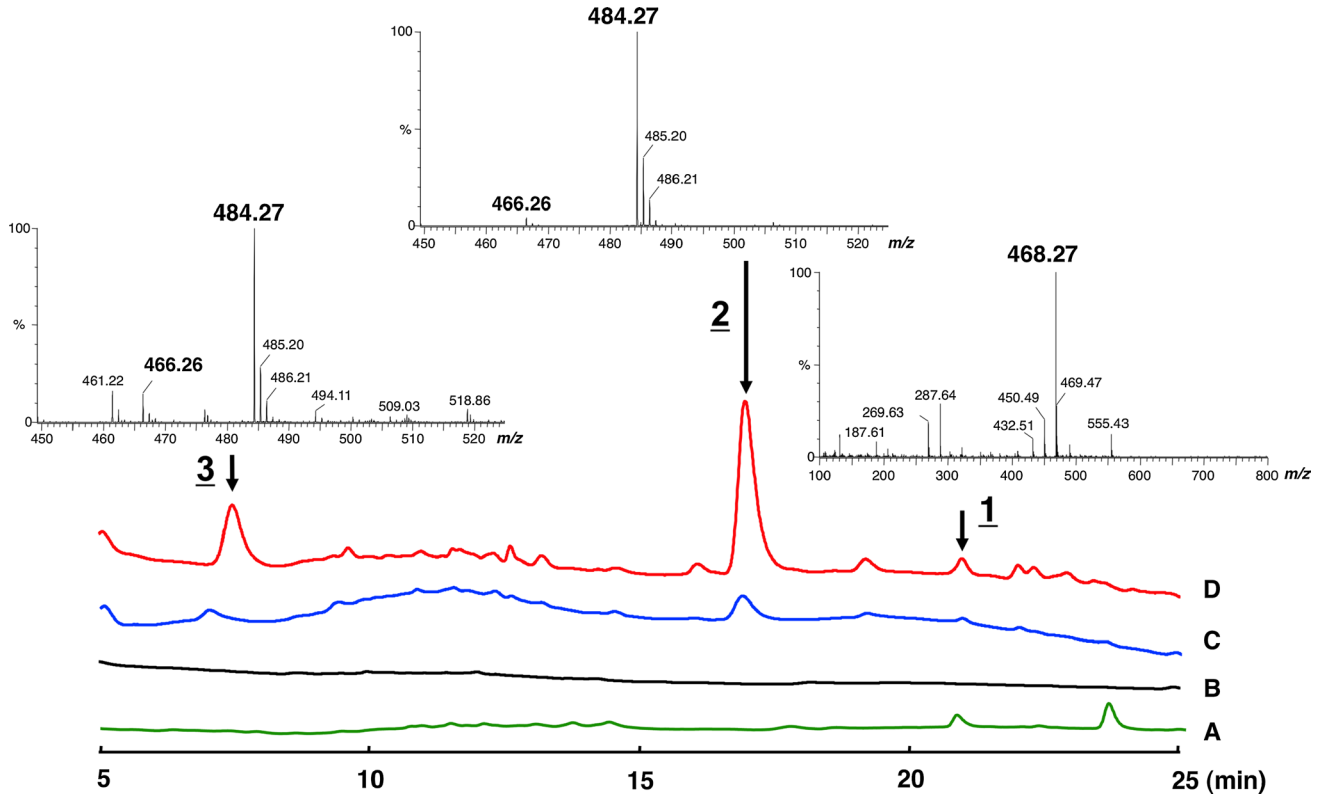

Fig. 3 HPLC analysis of the culture supernatant of the original producer *S. cyslabdanicus* K04-0144K04-0144 (*green line*) (*A*), *S. avermitilis* SUKA22 transformants carrying (*B*) pKU460 (vector control; *black line*), (*C*) pCLD101 harboring the entire *cld* cluster (*blue line*) and (*D*) pCLD102 harboring the entire *cld* cluster controlled by the constitutively expressed promoter (*rpsJp*) (*red line*). The whole culture was centrifuged to separate the mycelia. Three microliters of the culture supernatant was subjected to ODS HPLC (column; SHISEIDO MGII 3 µm, 2.0 × 100 mm, mobile phase; 30–95 v/v % CH_3CN in 0.05 w/v % formic acid for 30 min at 40 °C, flow rate; 0.2 ml/min, detection at 230 nm). Each peak fraction was analyzed by Q-TOF MS (Micromass, ABI)

the presence of a characteristic dehydration fragmentation peak at *m/z* 466 in **2** and **3**, respectively. The ^{1}H and ^{13}C NMR spectra of **2** and **3** were similar to that of **1** in Table 1. Analyses using ^{1}H–^{1}H correlation spectroscopy (COSY), ^{1}H–^{13}C hetero-nuclear multiple quantum coherence (HMQC) and ^{1}H–^{13}C hetero-nuclear multiple-bond connectivity (HMBC) revealed that **2** and **3** were the C-2 and C-17 hydroxyl derivatives of **1**, respectively (Fig. 4). Two pairs of correlations between two protons: H_1-2/H_3-19 and H_1-2/H_3-20 were observed by ^{1}H–^{1}H NOESY of **2**, suggesting that the hydroxyl residue at C-2 was equatorial. Three pairs of correlations between three protons: H_1-17/H_1-7, H_1-17/H_1-9, and H_1-17/H_1-3′ were observed by ^{1}H–^{1}H nuclear overhauser effect spectroscopy (NOESY) of **3**, suggesting that the C-17 residue was in a *S*-configuration. **1** and its hydroxylated derivatives (**2** and **3**) were produced as major metabolites by the heterologous expression of the *cld* cluster of *S. cyslabdanicus* K04-0144, suggesting that a set of four genes, *cldA-cldB-cldC-cldD*, was involved in the biosynthesis of **1**. The hydroxylated cyslabdans, **2** and **3**, by the heterologous expression of the *cld* gene cluster were not produced in the original producer *S. cyslabdanicus* K04-0144, suggesting that a putative hydroxylase was expressed from the genome of *S. avermitilis* SUKA22. Unfortunately, the potentiating effect of **2** and **3** on the activity of imipenem against MRSA was dramatically reduced. The introduction of hydroxyl residue in **1** might have an unfavorable effect on its activity.

Detection of the biosynthetic intermediate of 1 from culture mycelia

In our recent studies on bacterial terpene metabolites, most sesqui- and diterpene hydrocarbons and alcohols were found to be produced in mycelia of engineered heterologous host [40]. To identify an intermediate of **1**, metabolites in the culture mycelia of *S. avermitilis* SUKA22 transformants carrying pCLD102 were examined (Fig. 5). After cultivation of the transformants in the production medium, separated mycelia were extracted with methanol and the methanol extract was directly subjected to HPLC/MS. A new metabolite (**4**) was found in the mycelia, but not in the

Table 1 ^{1}H and ^{13}C NMR data of **1** and its hydroxylated derivatives, **2** and **3**

No.	**1**		**2**		**3**	
	δ_C (M)	δ_H (multi, *J* in Hz)	δ_C (M)	δ_H (multi, *J* in Hz)	δ_C (M)	δ_H (multi, *J* in Hz)
1	41.1 (t)	0.84 (2H, m)	39.4 (t)	0.90 (2H, m)	48.0 (t)	0.74 (1H, m) 1.96 (1H, m)
2	19.3 (t)	1.35 (1H, m) 1.63 (1H, m)	21.1 (t)	1.46 (1H, m) 1.62 (1H, m)	63.8 (d)	3.78 (1H, m)
3	43.0 (t)	1.14 (1H, m) 1.63 (1H, m)	41.7 (t)	1.22 (1H, m) 1.48 (1H, m)	50.1 (t)	1.09 (1H, m) 1.69 (1H, m)
4	34.1 (s)		32.6 (s)		32.5 (s)	
5	53.7 (d)	0.91 (1H, m)	52.0 (d)	1.06 (1H, m)	51.8 (d)	0.86 (1H, m)
6	27.8 (t)	1.63 (2H, m)	26.8 (t)	1.68 (2H, m)	26.0 (t)	1.58 (2H, m)
7	72.3 (d)	3.82 (1H, dd, $J = 4.5, 11.0$)	73.7 (d)	3.64 (1H, dd, $J = 4.5, 11.0$)	71.1 (d)	3.82 (1H, dd, $J = 4.5, 11.0$)
8	78.8 (s)		76.0 (s)		77.2 (s)	
9	55.2 (d)	1.35 (1H, m)	57.2 (d)	1.32 (1H, m)	53.7 (d)	1.33 (1H, m)
10	39.8 (s)		38.4 (s)		39.9 (s)	
11	24.4 (t)	2.13 (1H, m) 2.42 (1H, dt, $J = 6.5, 17.0$)	18.3 (t)	2.29 (1H, m) 2.55 (1H, dt, $J = 6.5, 17.0$)	23.2 (t)	2.13 (1H, m) 2.43 (1H, dt, $J = 6.5, 17.0$)
12	137.6 (d)	5.56 (1H, t, $J = 6.5$)	135.2 (d)	5.56 (1H, t, $J = 6.5$)	136.3 (d)	5.56 (1H, t, $J = 6.5$)
13	133.2 (s)		131.7 (s)		132.3 (s)	
14	143.1 (d)	6.35 (1H, dd, $J = 10.0, 10.0$)	140.2 (d)	6.34 (1H, dd, $J = 10.0, 10.0$)	141.9 (d)	6.33 (1H, dd, $J = 10.0, 10.0$)
15	110.0 (t)	4.86 (1H, d, $J = 10.0$) 5.03 (1H, dd, $J = 18.0$)	108.3 (t)	5.03 (1H, d, $J = 10.0$) 5.09 (1H, d, $J = 18.0$)	108.9 (t)	4.83(1H, d, $J = 10.0$) 5.03 (1H, dd, $J = 18.0$)
16	12.0 (q)	1.75 (3H, brs)	11.3 (q)	1.80 (3H, s)	10.8 (q)	1.78 (3H, s)
17	39.2 (t)	2.63 (1H, d, $J = 12.5$) 2.77 (1H, d, $J = 12.5$)	61.7 (d)	3.09 (1H, s)	37.7 (t)	2.62 (1H, d, $J = 12.5$) 2.76 (1H, d, $J = 12.5$)
18	34.0 (q)	0.91 (3H, s)	32.8 (q)	0.95 (3H, s)	33.9 (q)	0.94 (3H, s)
19	22.3 (q)	0.84 (3H, s)	23.6 (q)	0.92 (3H, s)	21.8 (q)	0.87 (3H, s)
20	16.0 (q)	1.00 (3H, s)	15.0 (q)	1.08 (3H, s)	15.5 (q)	1.02 (3H, s)
1′	177.4 (s)		175.1 (s)		176.5 (s)	
2′	55.8 (d)	4.41 (1H, dd, $J = 4.5, 8.0$)	54.6 (d)	4.72 (1H, dd, $J = 4.5, 8.0$)	54.2 (d)	4.40 (1H, dd, $J = 4.5, 8.0$)
3′	37.7 (t)	2.82 (1H, dd, $J = 8.0, 13.0$) 3.02 (1H, dd, $J = 4.5, 13.0$)	55.9 (t)	3.20 (1H, dd, $J = 8.0, 13.0$) 3.29 (1H, dd, $J = 4.5, 13.0$)	36.1 (t)	2.81 (1H, dd, $J = 8.0, 13.0$) 3.01 (1H, dd, $J = 4.5, 13.0$)
4′	172.5 (s)		170.3 (s)		171.4 (s)	
5′	22.8 (q)	1.98 (3H, s)	21.5 (q)	2.01 (3H, s)	21.5 (q)	1.97 (3H, s)

culture broth, whereas **1** and **2**, which were eluted at 0.76 and 1.01 min, respectively, were only observed in the culture broth (Fig. 5). The metabolite (**4**), which was eluted at 2.32 min with parent $[M + H]^+$ *m/z* 305, did not match the public MS databases. Fermentation products that were extracted with methanol from culture mycelia were purified by silica gel column chromatography. Approximately, 12 mg of the new compound (**4**) was obtained from 2 l of culture as a white amorphous powder. HR-MS (ESI) of **4** showed a molecular ion peak at *m/z* 305.2479 $[M + H]^+$, corresponding to $C_{20}H_{33}O_2$ (calcd. for 305.2475) for diterpene alcohol with five degrees of unsaturation. The ^{1}H and ^{13}C NMR spectra of **4** were similar to that of **1**, suggesting that **4** had a labdane skeleton (Fig. 6). The ^{1}H NMR spectrum of **4** showed two olefinic protons (δ_H 4.91, d, $J = 6.0$ Hz, 1H, H-15; 5.07, d, $J = 6.0$ Hz, 1H, H-15) assignable to an exomethylene. Additional olefinic protons (δ_H, 5.27, t, $J = 6.5$ Hz, 1H, H-12; 6.28, dd, $J = 10.0$, 18.0 Hz, 1H, H-14) were observed. An analysis of ^{13}C NMR and distortionless enhancement by polarization transfer (DEPT) spectra of **4** showed 20 resolved signals and confirmed the presence of four methyls, six sp^3 methylenes, one sp^2 methylene, three sp^3 methines, two sp^2 methines, one sp^2, and three sp^3 quaternary carbons. An analysis of ^{1}H–^{1}H COSY revealed four partial structures: C-1–C-3, C-5–C-7, C-8–C-12, and C-14–C-15, and the ^{1}H–^{13}C long-range couplings of *2J* and *3J* observed in the ^{1}H–^{13}C HMBC experiments gave the following information: the cross peaks from H_3-20 (δ_H 0.88) to C-1 (δ_C 39.3), C-5 (δ_C 52.4), C-9 (δ_C 52.3), and C-10 (δ_C 39.4), H_3-18 (δ_H 0.85) to C-3 (δ_C 41.9), C-4 (δ_C 33.5), C-5, and C-19 (δ_C 33.4), H_3-19 to C-3, C-4, C-5, and C-18 (δ_C 21.7), H_2-6 (δ_H 2.05)

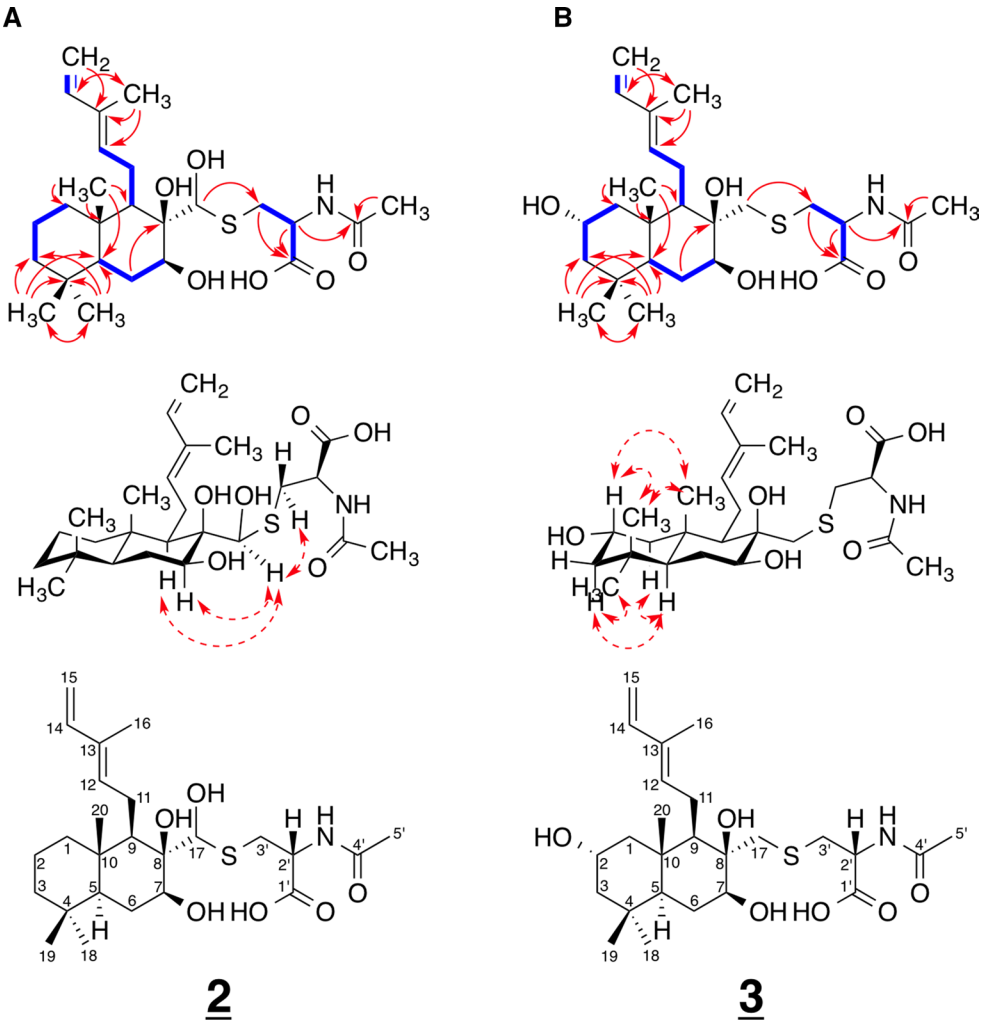

Fig. 4 Structure of 17-hydroxycyslabdan A (**a**; **2**) and 2-hydroxycyslabdan A (**b**; **3**) produced by *S. avermitilis* SUKA22 carrying pCLD102. The *upper panel* shows ^{1}H–^{1}H COSY (*bold blue line*) and ^{1}H–^{13}C HMBC (*red arrow*), and the *middle panel* is ^{1}H–^{1}H NOESY (*dashed arrow*) data for each compound. *Double arrows* indicate a cross peak in ^{1}H–^{13}C HMBC

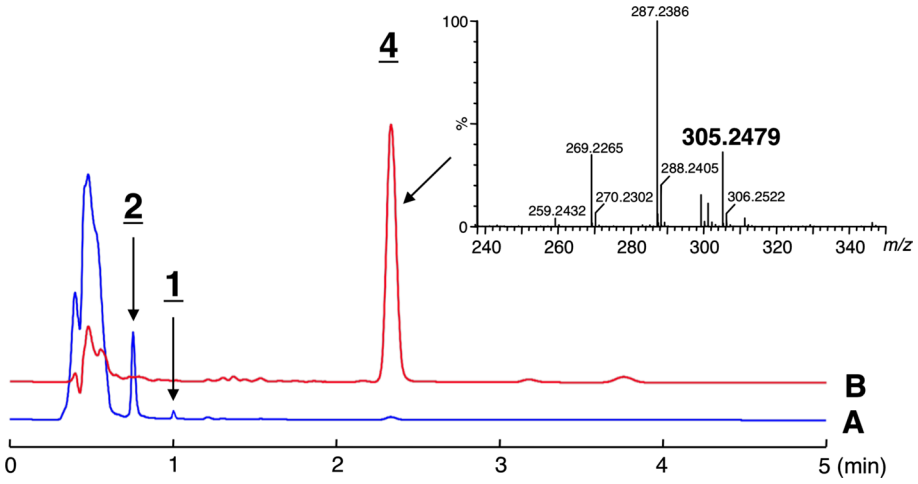

Fig. 5 HPLC analysis of the culture supernatant (*blue line*) (*A*) and methanol extract from mycelia (*red line*) (*B*) of *S. avermitilis* SUKA22 carrying pCLD102, and ESI–MS fragmentation of peak **4**. The mycelia obtained from 10 ml of the culture were extracted with 5 ml of methanol. Five microliters of the culture supernatant or methanol extract of mycelia was directly subjected to ODS HPLC (*column*; Waters, BEH C18 1.7 µm, 2.1 × 100 mm, mobile phase; 70 v/v % CH_3CN in 0.05 w/v % formic acid at 40 °C, flow rate; 0.2 ml/min, detection at 230 nm)

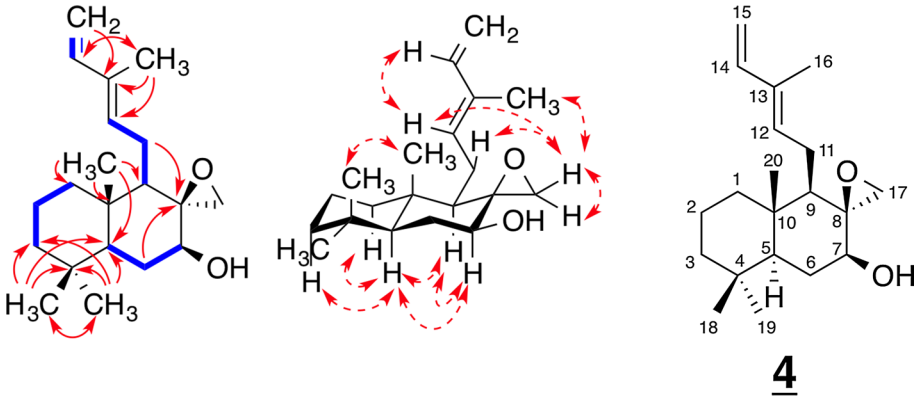

Fig. 6 Structure of (*7S, 8S, 12E*)-8,17-epoxy-7-hydroxy-labda-12,14-diene (**4**) produced by *S. avermitilis* SUKA22 carrying pCLD102. The *upper panel* shows ^{1}H–^{1}H COSY (*bold blue line*), ^{1}H–^{13}C HMBC (*red arrow*), and ^{1}H–^{1}H NOESY (*dashed arrow*) data for each compound. *Double arrows* indicate a cross peak in ^{1}H–^{13}C HMBC

NMR chemical shifts in $CDCl_3$

No.	δ_C (M)	δ_H (multi, *J* in Hz)
1	39.3 (t)	0.92 (1H, m), 1.78 (1H, m)
2	18.6 (t)	1.43 (1H, m), 1.60 (1H, m)
3	41.9 (t)	1.17 (1H, m), 1.33 (1H, m)
4	33.5 (s)	-
5	52.4 (d)	1.04 (1H, m)
6	30.7 (t)	1.37 (1H, m), 2.05 (1H, m)
7	69.3 (d)	3.68 (1H, m)
8	60.1 (s)	-
9	52.3 (d)	1.46 (1H, m)
10	39.4 (s)	-
11	20.8 (t)	1.82 (1H, m), 2.05 (1H, m)
12	134.8 (d)	5.27 (1H, t, *J* = 6.5)
13	134.0 (s)	-
14	141.5 (d)	6.28 (1H, dd, *J* = 10.0, 18.0)
15	110.7 (t)	4.91 (1H, d, *J* = 10.0), 5.07 (1H, d, *J* = 18.0)
16	12.2 (q)	1.71 (3H, s)
17	45.2 (t)	2.48 (1H, d, *J* = 6.0), 2.87 (1H, d, *J* = 6.0)
18	21.7 (q)	0.85 (3H, s)
19	33.4 (q)	0.90 (3H, s)
20	14.7 (q)	0.88 (3H, s)

to C-8 (δ_C 60.1), H_2-11 (δ_H 2.05) to C-8, H_3-16 to C-12 (δ_C 134.8), C-13 (δ_C 134.0), and C-14 (δ_C 141.5), H_1-14 (δ_H 6.28) to C-16 (δ_C 12.1), and H_3-15 (δ_H 5.07) to C-13 supported the structure shown in Fig. 6. In consideration of the five degrees of unsaturation and the ^{13}C NMR chemical shifts of **4**, the carbon chemical shifts at δ 60.1 (C-8) and 45.2 (C-17) were assigned to epoxy carbons instead of the characteristic tertiary hydroxyl carbon signal at δ 78.8 (C-8) and sp^3 methylene carbon at δ 39.2 (C-17) of **1**. The stereochemical assignments of the methylene protons (H_2-17) were elucidated from the ^{1}H–^{1}H NOESY spectrum of **4**. Three pairs of correlations between two protons H_2-17/H_3-16, H_2-17/H_1-12, and H_2-17/H_2-11, respectively, were observed by ^{1}H-^{1}H NOESY, suggesting that the epoxy oxygen at C-8 was assigned an axial configuration (Fig. 6). The hydroxyl residue at C-7 was assigned an equatorial configuration based on the observed correlations between two protons H_1-7 with H_1-9 and H_1-6. The absolute configuration was then assigned with confidence based on the derivation from the labdane-type bicyclic diterpene, giving the assignment of **4** as (*7S, 8S, 12E*)-8,17-epoxy-7-hydroxylabda-12,14-diene (Fig. 6).

Properties of CldB, CldC, and CldD

Based on the predicted function of each gene product: CldA, CldB, CldC or CldD, the biosynthetic process was expected as follows: CldA catalyzes the generation of GGPP by condensation of one molecule of dimethylallyl diphosphate (DMAPP) and three molecules of isopentenyl diphosphate (IPP). CldD (presumptive labdatriene synthase) and CldB (presumptive (+)-copalyl diphosphate synthase),

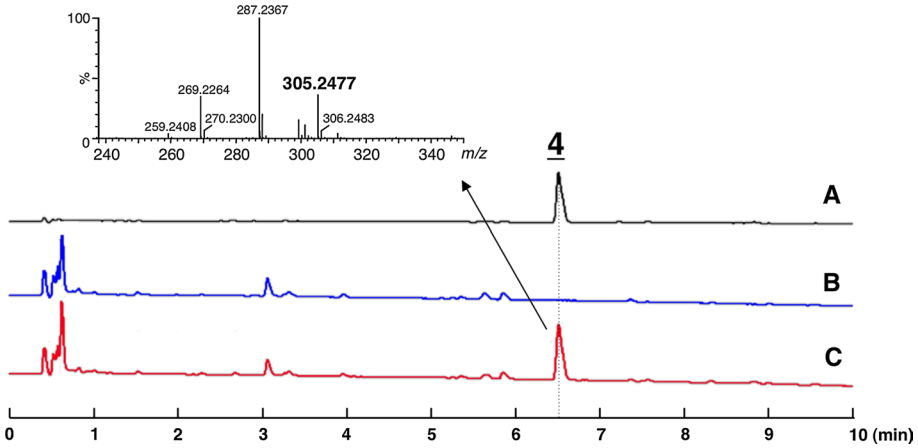

Fig. 7 HPLC analysis of bioconversion products of *S. avermitilis* SUKA22 carrying *cldC* controlled by the constitutively expressed promoter and ESI–MS fragmentation of the conversion product eluted at 6.51 min. An authentic sample of **4** (*black line*) (*A*), whole culture extract of *S. avermitilis* SUKA22 carrying *cldC* without (*blue line*) (*B*) and with (*red line*) (*C*) the substrate (**5**). *S. avermitilis* SUKA22 carrying *cldC* was grown in medium (4 g of yeast extract, 10 g of malt extract, and 4 g of glucose, pH 7.0) at 28 °C with shaking. After a 24-h cultivation, **5** (dissolved in methanol) was added to a final concentration of 10 µg/ml and the culture was continued for an additional 48 h. An equal volume of methanol was added and the mycelia were removed by centrifugation. Five microliters of the methanol extract was subjected to HPLC/MS (*column*; Waters, BEH C18 1.7 µm, 2.1 × 100 mm, mobile phase; 30–95 v/v % CH_3CN in 0.05 w/v % formic acid for 10 min at 40 °C, flow rate; 0.2 ml/min, detection at 230 nm)

which are type-A and -B terpene synthases, respectively, catalyze the generation of labda-8(17),12(*E*),14-triene from GGPP, in which (+)-copalyl diphosphate is generated by CldB. (+)-Copalyl diphosphate is then converted to labda-8(17),12(*E*),14-triene by CldD. Since a set of three genes: *cldA*, *cldB*, and *cldD*, may be involved in the formation of labda-8(17),12(*E*),14-triene, an in-frame deletion of *cldC* in the *cld* cluster (*cldA-cldB-cldC-cldD*) was prepared by λ-RED recombination and the resultant recombinant plasmid pCLD104 was introduced into the engineered strain *S. avermitilis* SUKA22. After cultivation of transformants carrying pCLD104, mycelia were extracted with methanol and the methanol extract was directly subjected to GC–MS. The metabolite (**5**) eluted at 10.76 min with parent $[M]^+$ *m/z* 272 was observed, whereas other diterpene metabolites were not detected in the culture broth or mycelia (Fig. S1). Approximately, 20 milligrams of **5** was obtained from 2 l of culture as transparent oil. Ultimately, **5** was identical to known diterpene hydrocarbon, labda-8(17),12(*E*),14-triene (biformene; from heartwood of *Dacrydium biforme*), by comparisons with ^1H and ^{13}C NMR spectra [7] (Fig. S2).

Transformants carrying pCLD102 (*cld* cluster) produced **1** and its derivatives, **2** and **3**, in culture broth and **4** in the mycelia, while transformants carrying pCLD104, which was one of the derivatives of pCLD102 by the in-frame deletion of the *cldC* gene from the *cld* cluster (*cldA-cldB-cldC-cldD*), accumulated only a single component, the diterpene hydrocarbon **5**. These results indicated that CldC was involved in the conversion of **5**–**4**. These structures suggested that the formation of **4** from **5** required two successive oxidation reactions, hydroxylation and epoxidation, respectively. To confirm the predicted biochemical function of the CldC protein, the recombinant protein was expressed using a standard *Escherichia coli* T7-RNA polymerase-based expression host-vector system. However, N-terminal and/or C-terminal His_6-tagged CldC were initially obtained as inclusion bodies. Biochemical function was examined by the bioconversion of **5** in *S. avermitilis* SUKA22 transformants carrying constitutively expressed *cldC*. As shown in Fig. 7, transformants carrying *cldC* controlled by the *rpsJ* promoter converted **5**–**4**, suggesting that the cytochrome P450, CldC, catalyzed two successive oxidation reactions: hydroxylation at C-7 and epoxidation at C-8,17 exomethylene. Thus, the final reaction product by four gene products (CldA, CldB, CldC, and CldD) of the *cld* cluster was defined as **4**.

Mca-deletion mutants failed to produce 1

A set of four genes: *cldA*, *cldB*, *cldC* and *cldD* were found to be involved in the formation of **4** in the present study. The next step was to elucidate the mechanism underlying the formation of **1** from **4**. Some epoxy derivatives are toxic against organisms because they are more reactive compounds. Mycothiol (MSH) is the primary low-molecular-weight thiol in most actinomycetes and its biological functions have been examined extensively in mycobacteria, in which it is involved in the detoxification of exogenous xenobiotic agents. Mycobacteria rely on MSH for protection against electrophilic toxins such as alkylating agents,

halogens, and epoxide derivatives. The MSH-dependent detoxification system utilizes nucleophilic reactions to conjugate MSH and toxins through the sulfur group of MSH forming an *S*-conjugate. Ultimately a single enzymatic activity, which is involved in the specific amidase (MSH-*S*-conjugate amidase), produces a mercapturic acid derivative (*N*-acetylcysteinyl) from the *S*-conjugate by releasing a 1D-*myo*-inositol-2-amino-2-deoxylglucopyranoside residue (GlcN-Ins). To investigate the involvement of MSH in the formation of **1** from **4**, an in-frame deletion mutant of the gene encoding MSH-*S*-conjugate amidase (*mca*; a gene product is 32.8 kDa; SAV_3299) was constructed by allelic replacement.

The morphological properties and growth rates of all *mca* mutants of *S. avermitilis* SUKA22 were similar to those of the parent strain. After the introduction of pCLD102 into *S. avermitilis* SUKA22 *Δmca*, the culture broth and methanol extract of the mycelia of transformants were analyzed by HPLC/MS. Although **1** was produced in the culture broth of the parent transformants (*S. avermitilis* SUKA22 carrying pCLD102), none of the *mca* mutants carrying pCLD102 produced **1** (Fig. 8a). To confirm the accumulation of the intermediate **4**, the methanol extract of mycelia was analyzed by HPLC. All *mca* mutants carrying pCLD102 accumulated **4** to the same level as that of *S. avermitilis* SUKA22 carrying pCLD102 (Fig. 8b). Furthermore, a peak (**6**), which was eluted at 2.95 min (the parent molecular ion peak of the fraction eluted at 3.07 min was bigger than *m/z* 791), was observed in not only the parent *S. avermitilis* SUKA22 carrying pCLD102, but also its *mca*-deletion mutants carrying pCLD102 (Fig. 9a). The corresponding peak was detected in the culture broth and mycelia; however, it accumulated more in the culture broth than in the mycelium (Fig. 9b). HR-MS (ESI) of **6** showed a molecular ion peak at *m/z* 791.3975 $[M + H]^+$, corresponding to $C_{37}H_{63}N_2O_{14}S$ (calcd. for 791.3995) for the MSH-*S*-conjugate (**6**). Thus, these results suggested that the parent and *Δmca* mutant strains carrying pCLD102 both accumulated the MSH-*S*-conjugate (**6**). However, since *Δmca* transformants carrying pCLD102 did not possess the ability to hydrolyze the MSH-*S*-conjugate, the transformants did not produce **1** (Fig. 10).

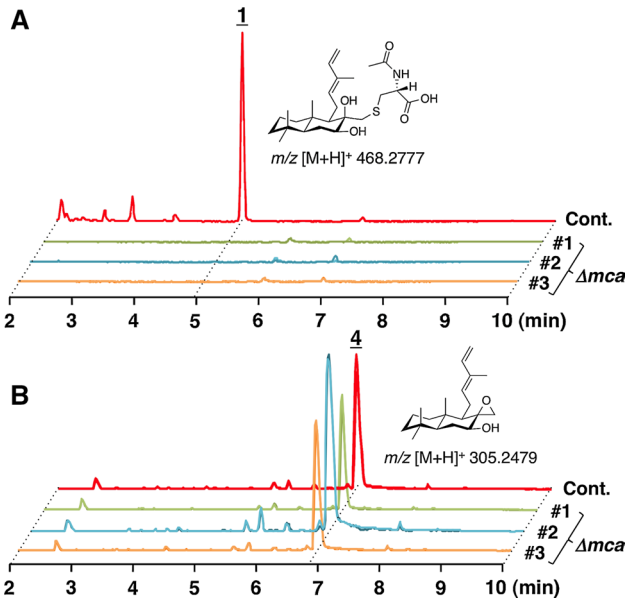

Fig. 8 HPLC analysis of metabolites in the culture broth (**a**) and mycelia (**b**) of *S. avermitilis* SUKA22 or its *Δmca* carrying pCLD102. Five microliters of the supernatant or methanol extract of mycelia was subjected to HPLC/TofMS (*column*; Waters, BEH C18 1.7 µm, 2.1 × 100 mm, mobile phase; 30–90 v/v % CH_3CN in 0.05 w/v % formic acid for 10 min at 40 °C, flow rate; 0.2 ml/min, detection at *m/z* 468 (**a**) or *m/z* 305 (**b**), respectively). Abbreviations are as follows; Cont. indicates *S. avermitilis* SUKA22 carrying pCLD102 (*red line*), and #1 to #3 are *S. avermitilis* SUKA22 *Δmca* carrying pCLD102 clones #1 to #3 (*yellow-green*, *blue-green*, and *orange lines*)

Streptomyces anulatus GM95 harbored a *cld*-like gene cluster

We determined whether other *Actinomycetales* microorganisms harbored the *cld* or a similar gene cluster. Our in-house draft genome databases showed that *S. anulatus* GM95 had a similar gene cluster (*rmn* cluster: accession # LC064029) that was composed of four genes encoding the presumptive GGPP synthase, type-B terpene synthase, and cytochrome P450 and type-A terpene synthases (Fig. 2). Genes that formed an operon upstream of the gene cluster were similar to those of *S. cyslabdanicus* K04-0144, five genes in this operon were translationally coupled with the downstream gene, and the first four genes were the same as a set of the multi-component regulatory system that is frequently found in *Streptomyces* genomes [20, 37]. Although we expected the production of **1** or its related metabolites from *S. anulatus* GM95, the microorganism did not produce any diterpene metabolites under any culture conditions, suggesting that the gene cluster was silent in this microorganism.

The predicted 360-aa gene product of *rmnA* of *S. anulatus* GM95, which is the first gene in the operon, showed 57 % identity and 70 % positive matches to *S. cyslabdanicus* K04-0144 CldA (361-aa; GGPP synthases). The deduced GGPP synthase, RmnA, consisted of the universally conserved two divalent metal-binding motifs, acidic amino acid-rich ^{95}H**DD**VM**D** and the downstream ^{241}AFQLR**DD**L. The predicted 549-aa gene product of *rmnB* downstream of *rmnA* showed 55 % identity and 65 % positive matches to *S. cyslabdanicus* K04-0144 CldB (532-aa; type-B terpene synthase). The motifs DxDDTA and QxxDGSW in copalyl

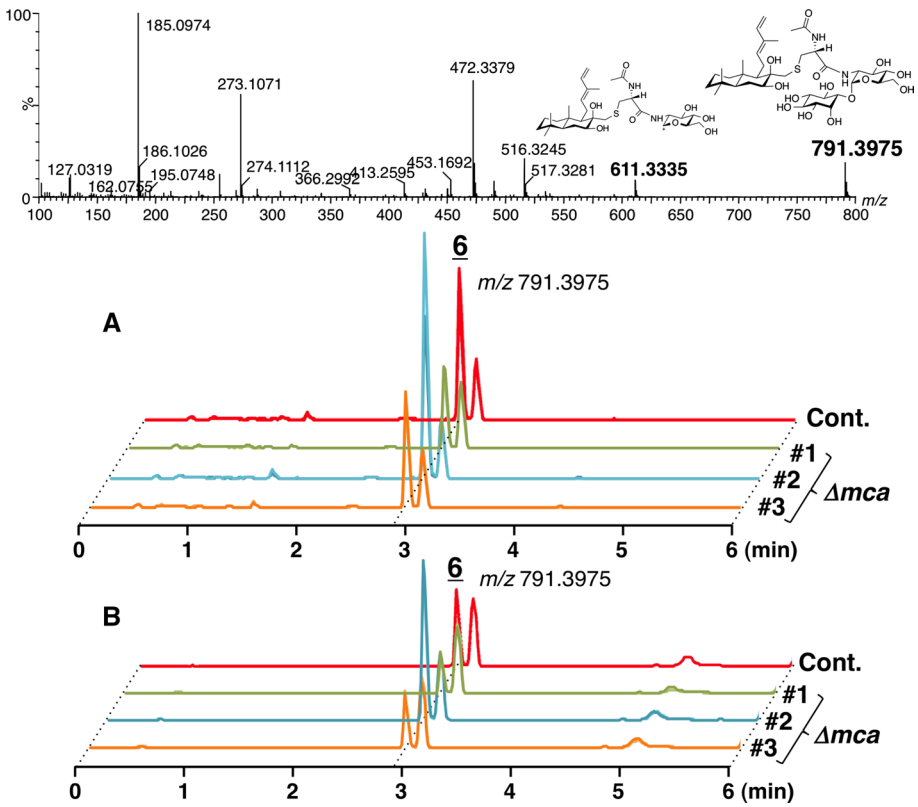

Fig. 9 HPLC analysis of metabolites in the culture broth (**a**) and mycelia (**b**) of *S. avermitilis* SUKA22 or its *Δmca* carrying pCLD102. Analytical conditions were the same as those described in Fig. 8. A chromatogram was traced at *m/z* 791. The *upper panel* shows the ESI–MS fragmentation of a peak (**6**) eluted at 2.92 min of clone #1. Abbreviations are the same as those in Fig. 8

diphosphate synthases were conserved in the RmnB product (^{313}**DTDDTA**, ^{443}**QSDDGSW**). The predicted 452-aa gene product of *rmnC* downstream of *rmnB* showed 66 % identity and 79 % positive matches to *S. cyslabdanicus* K04-0144 CldC (454-aa; cytochrome P450). The universally conserved cysteine residue found in the C-terminal region of all cytochrome P450 s and that binds to the proximal face of the protoheme co-factor was found in RmnC (-RM**C**IG-) at ^{393}Cys. The last predicted 322-aa gene product of *rmnD* downstream of *rmnC* showed 53 % identity and 63 % positive matches to *S. cyslabdanicus* K04-0144 CldD (329-aa; type-A terpene synthase). The genes *rmnA* and *rmnC* of *S. anulatus* GM95 were translationally coupled to the downstream genes *rmnB* and *rmnD*, respectively. The deduced type-A terpene synthase, RmnD, displayed the universally conserved pair of divalent metal-binding motifs, an acidic amino acid-rich ^{93}**DD**AHG**E**, and the downstream triad ^{234}**N**DLA**S**YAK**E**.

We expected the production of labdane-type diterpene metabolites by the heterologous expression of the *rmn* cluster of *S. anulatus* GM95 using engineered *S. avermitilis* SUKA22. A set of the gene cluster consisting of four genes of *S. anulatus* GM95 was cloned from the chromosomal DNA by the λ-RED system based on recombination between short homologous regions. Since a biosynthetic gene cluster was silent in the original strain, *S. anulatus* GM95, a specific promoter sequence was introduced upstream of the first gene in the gene cluster. At least five peaks were observed in the methanol extract of mycelia from transformants carrying pRMN102 (Fig. S3). Of these, a peak eluted at 6.52 min was identical to **4** by a comparison with an authentic sample of **4**. Two peaks that were eluted at 2.78 min (**8**) and 7.22 min (**7**) were obtained at 7 and 12 mg, respectively, from a 2-l culture. The ^{1}H and ^{13}C NMR data of **7** were identical to those of the plant (*Nicotiana raimondii*) diterpene metabolite, raimonol [30] (Fig. S4). A comparative analysis of ESI–MS fragments between **7** and **8** indicated that **8** was a simple hydroxylation product of **7** based on characteristic dehydration fragmentation. The HR-MS (ESI) of **8** showed a molecular ion peak at *m/z* 305.2497 $[M + H]^+$, which was consistent with the molecular formula of $C_{20}H_{33}O_2$ (calcd. for 305.2475) for a dihydroxy diterpene with five degrees of unsaturation. The ^{1}H–^{13}C HMQC and ^{1}H–^{13}C HMBC of **8** revealed C-2 alcohol derivative of **7**. Two pairs of correlations between two protons: H_1-2/H_3-18 and H_1-2/H_3-20, were observed by ^{1}H–^{1}H NOESY, suggesting that the hydroxyl residue at C-2 was equatorial (Fig. S4). Another two peaks: **9** (eluted at 3.52 min) and **10** (eluted at 2.16 min), could not be purified to a sufficient amount for a spectrum analysis; however, an analysis of their MS fragmentation showed that they were derivatives of the oxidation of **8** and hydroxylation of **4**, respectively (Fig. 9).

Discussion

Terpenoid metabolites are generally considered to be the major metabolites of plants or fungi; however, only a minor fraction of these widely occurring metabolites has been identified in bacterial origins. Extensive bacterial genome sequencing and bioinformatic analyses of deduced bacterial proteins have recently identified more than 260 distinct predicted terpene synthases [40]. These findings indicate that the genes encoding these terpene synthases are widely distributed in bacteria. The majority of these presumptive terpene synthases are most likely sesquiterpene synthases and the group of diterpene synthases was a small fraction. A bioinformatic analysis of deduced proteins using a profile based on a hidden Markov model generated from bacterial protein databases revealed that *S. cyslabdanicus* K04-0144, which produced **1**, harbored at least three genes encoding terpene synthases. Two of these were the predicted sesquiterpene synthases, geosmin and *epi*-isozizaene synthases, which are often detected in the genomes of *Actinomycetales* microorganisms. Plant and fungal diterpene synthases have been classified into at least four groups based on the combination of two fundamental types of cyclization reactions [39]: (1) type-A, (2) type-B, (3) type-A/type-B, and (4) type-B/type-A. Type-B synthases catalyze the initiation of cyclization by protonation at the C14,15-double bond of GGPP, which is distal to the allylic diphosphate. The type-A synthase reaction is then initiated by ionization of the diphosphate of GGPP to give an allylic cation, followed by deprotonation to generate olefinic diterpene hydrocarbons or the capture of a water molecule to generate a diterpene alcohol. To date, three pairs of type-B/type-A diterpene synthases have been characterized in the terpentecin biosynthesis of *Kitasatospora griseola* MF730-N6 (terpentedienyl diphosphate synthase; BAB39206/terpentetriene synthase; BAB39207), viguiepinol biosynthesis of *Streptomyces* sp. KO-3988 (*ent*-copalyl diphosphate synthase; BAD86797/pimaradiene synthase; BAD86798), and oxaloterpin biosynthesis of *S. griseus* CB00830 (*ent*-copalyl diphosphate synthase; AHK61132/pimaradiene synthase; AHK61133). Biochemical function analyses revealed that two pairs of type-B/type-A enzymes, BAB39206/BAB39207 and BAD86797/BAD86798 (or AHK61132/AHK61133), generated the bicyclic diterpene hydrocarbon, terpente-3,13,15-triene, and tricyclic diterpene hydrocarbon, pimara-9(11),15-diene, respectively. Labdane-type diterpene metabolites (**1**, **2**, **3**, **7**, and **8**) were produced by the heterologous expression of the *cld* cluster of *S. cyslabdanicus* K04-0144 or *rmn* cluster of *S. anulatus* GM95 in an engineered *S. avermitilis*, suggesting that CldB/CldD and RmnD/RmnB pairs were involved in the generation of the labdane-type bicyclic diterpene hydrocarbon, labda-8(17),12(*E*),14-triene (Fig. 10); however, this has yet to be demonstrated directly. Two conserved divalent metal-binding motifs, an acidic amino acid-rich -DDxx[DE]- or -DDxxx[DE]- and the more conventional downstream triad Nxxx[ST]xxx[DE] are present in all type-A synthases: BAB39207, BAD86798, AHK61133, CldD, and RmnD. Terpentetriene synthase (BAB39207) and pimaradiene synthase (BAD86798 and AHK61133) both possess the characteristic acidic amino acid-rich motif -DDxx[DE]-, whereas the -DDxxxE- motif was observed

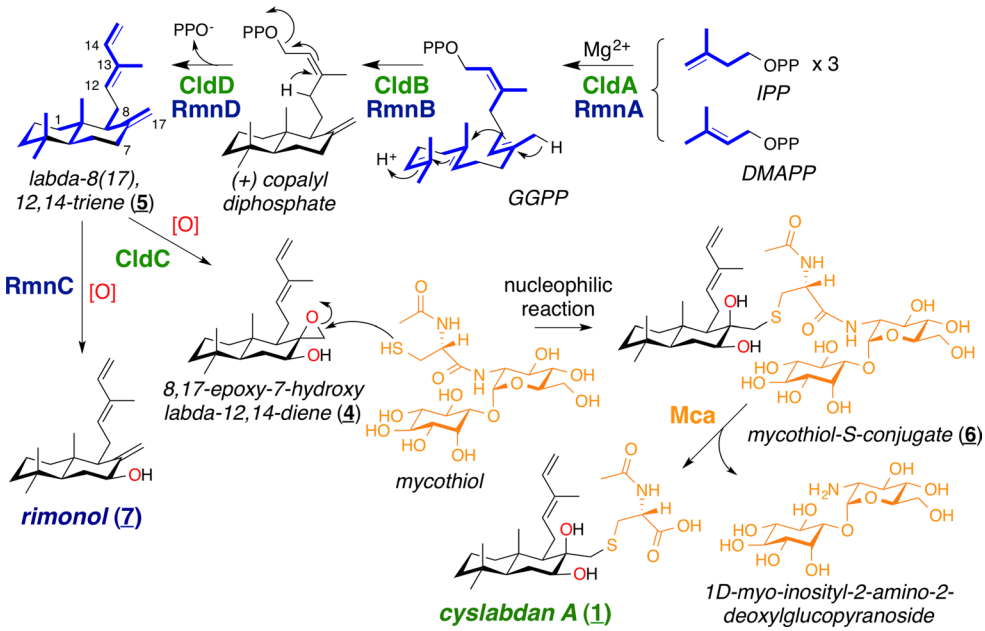

Fig. 10 Proposed biosynthetic pathway of labdane-type bicyclic diterpene metabolites, cyslabdan A (**1**) and raimonol (**7**)

in CldD and RmnD, which are predicted to be labdatriene synthases (Fig. S5). Bacterial type-A terpene synthases display one of the conserved metal-binding motifs, the triad sequence -NxxxSxxxE-, found in the C-terminal region, whereas the downstream triad -NxxxTxxxE- is present in both pimaradiene synthases (BAD86798 and AHK61133). On the other hand, two motifs of type-B synthases, the acid amino acid-rich motif -DxDDT[AS]- and downstream motif -QxxDGSW-, were present and conserved in all type-B synthases (Fig. S5).

The results obtained regarding the expression of the *cld* cluster of *S. cyslabdanicus* K04-0144 indicated that at least four genes: *cldA*, *cldB*, *cldC*, and *cldD*, were required for the production of **1** in the heterologous host. However, an analysis of metabolites in the mycelia expressing the cluster indicated that the biosynthetic products of these four gene products were identical to **4**, but not to **1**. This speculation has been supported by the function of CldC, which is a bifunctional cytochrome P450 protein. The bioconversion of **5** using an engineered *S. avermitilis* carrying the constitutively expressed *cldC* gene gave the same product as **4**, suggesting that the epoxidation of a double bond at C-8(17) and hydroxylation at C-7 of **5** were both performed by CldC. Thus, the biosynthetic process by four gene products was as follow: (1) CldA catalyzes the generation of GGPP from IPP and DMAPP in the presence of magnesium ions. (2) GGPP is converted to (+)-copalyl diphosphate by CldB. (3) CldD catalyzes the generation of labdane-type bicyclic diterpene hydrocarbon **5**. (4) **5** is hydroxylated and epoxidated by the bifunctional enzyme CldC to generate **4** (Fig. 10). The production of **7** by the *rmn* cluster appeared to be similar to *cld* biosynthesis because the composition of the biosynthetic genes in the *rmn* cluster was the same as that in the *cld* cluster. A difference between the biosynthesis of *cld* and *rmn* may be the substrate specificity of the cytochrome P450 enzymes, CldC and RmnC. Since the efficiency of the epoxidation activity of RmnC was markedly lower than that of CldC, an olefine between C-8 and C-17 remained and **5** (generated from IPP and DMAPP by RmnA, RmnB, and RmnD) was mainly converted to **7** by RmnC (Fig. 10). A very small amount of **4** was detected in mycelia by the trace reaction of RmnC.

In many organisms, low-molecular-weight thiols participate in a number of important biological functions as redox buffers and reducing cofactors, and also in xenobiotic detoxification. Among different organisms, the thiols utilized for such purposes are structurally diverse such as the tripeptide glutathione [10, 19] in eukaryotes and Gram-negative bacteria or the cysteinyl pseudo-disaccharide MSH in *Actinomycetales* microorganisms [18, 29]. A more efficient detoxification pathway is utilized by actinomycetes, in which a single enzyme, MSH-*S*-conjugate amidase (Mca), hydrolyzes the glucosaminyl–amide bond of MSH-*S*-conjugates to liberate the mercapturic acid-labeled component and GlcN-Ins [33]. The mercapturic acid derivatives are then exported from the cell and the liberated GlcN-Ins is recycled back into the MSH biosynthetic pathway [2, 4, 28]. The broad hydrolytic activity of the MSH-*S*-conjugate by *mca* may play an important role in MSH-dependent secondary metabolite detoxification during its biosynthesis, suggesting that the mercapturic acid derivatives of metabolites are exported in the culture broth of the producing microorganism. The results obtained in the present study revealed that the gene products of four genes: *cldA*, *cldB*, *cldC*, and *cldD*, of the *cld* cluster catalyzed the generation of **4** from IPP and DMAPP through GGPP, labda-8(17),12(*E*),14-triene, and **4**. Labdane-type diterpene, **4**, accumulated in the mycelia, but was not exported in the culture broth. In both strains, *S. cyslabdanicus* K04-0144 and *S. avermitilis* SUKA22, **4** was converted to the MSH-*S*-conjugate (**6**), which may have occurred through a non-enzymatic nucleophilic reaction with MSH. Although the excretion system of mercapturic acid derivatives in *Actinomycetales* microorganisms currently remains unclear, **1** (the mercapturic acid derivative of **4**) by MSH-*S*-conjugate amidase, which is a gene product of *mca*, may have been efficiently excreted from the mycelia. Since orthologs of *mca* and genes involved in the biosynthesis of MSH (*mshA*, *mshB*, *mshC*, and *mshD*) were detected in *S. cyslabdanicus* K04-0144, similar to *S. avermitilis* (*mca*; *sav3299*, *mshA*; *sav4006*, *mshB*; *sav3138*, *mshC*; *sav6647*, and *mshD*; *sav4058*), the producing microorganism may also have the ability to convert **4**–**1** through the MSH-*S*-conjugate (**6**). Thus, **1** was produced in the culture broth by the excretion of the epoxide derivative of the labdane-type diterpene metabolite (**4**) using MSH-mediated xenobiotic detoxification. Similar findings would be also observed in other secondary metabolite production processes such as those for seongomycin [5], naphthomycin J [13], and lactacystin [32].

Acknowledgments We thank Y. Yamada and T. Uchiyama for their technical assistance in this study. This work supported by a research Grant-in-Aid for Scientific Research on Innovative Areas from the Ministry of Education, Culture, Sports, Science and Technology of Japan (to H.I.), and a research Grant-in-Aid for "Project focused on developing key technology of discovering and manufacturing drug for next-generation treatment and diagnosis" from the Ministry of Economy, Trade and Industry of Japan (to K.S. and H.I.).

References

1. Albert H, Dale EC, Lee E, Ow DW (1995) Site-specific integration of DNA into wild-type and mutant lox sites placed in the plant genome. Plant J 7:649–659
2. Anderberg S, Newton GL, Fahey RC (1998) Mycothiol biosynthesis and metabolism: cellular levels of potential intermediates in the biosynthesis and degradation of mycothiol. J Biol Chem 273:30391–30397

3. Bohlmann J, Meyer-Gauen G, Croteau R (1998) Plant terpenoid synthases: molecular biology and phylogenetic analysis. Proc Natl Acad Sci USA 95:4126–4133
4. Bohme CC, Arscott LD, Becker K, Schirmer RH, Williams CH Jr (2000) Kinetic characterization of glutathione reductase from the malarial parasite *Plasmodium falciparum*. Comparison with the human enzyme. J Biol Chem 275:37317–37323
5. Camery JR, Hong S-T, Gould SJ (1997) Seongomycin: a new sulfur-containing benzo[b]fluorene derived from genes clustered with those for kanamycin biosynthesis. Tetrahedron Lett 38:3139–3142
6. Cane DE, He X, Kobayashi S, Omura S, Ikeda H (2006) Geosmin biosynthesis in *Streptomyces avermitilis*. Molecular cloning, expression, and mechanistic study of the germacradienol/geosmin synthase. J Antibiot 59:471–479
7. Carman RM, Grant PK (1961) Biformene. J Chem Soc 1961:2187–2191
8. Dairi T, Hamano Y, Kuzuyama T, Itoh N, Furihata K, Seto H (2001) Eubacterial diterpene cyclase genes essential for production of the isoprenoid antibiotic terpentecin. J Bacteriol 183:6085–6094
9. Datsenko KA, Wanner BL (2000) One-step inactivation of chromosomal genes in *Escherichia coli* K-12 using PCR products. Proc Natl Acad Sci USA 97:6640–6645
10. Franco R, Schoneveld OJ, Pappa A, Panayiotidis MI (2007) The central role of glutathione in the pathophysiology of human diseases. Arch Physiol Biochem 113:234–258
11. Fukumoto A, Kim Y-P, Matsumoto A, Takahashi Y, Shiomi K, Tomoda H, Omura S (2008) Cyslabdan, a new potentiator of imipenem activity against methicillin-resistant *Staphylococcus aureus*, produced by *Streptomyces* sp. K04-0144 I. Taxonomy, fermentation, isolation and structural elucidation. J Antibiot 61:1–6
12. Fukumoto A, Kim Y-P, Hanaki H, Shiomi K, Tomoda H, Omura S (2008) Cyslabdan, a new potentiator of imipenem activity against methicillin-resistant *Staphylococcus aureus*, produced by *Streptomyces* sp. K04-0144 II. Biological activities. J Antibiot 61:7–10
13. Hooper AM, Rickards RW (1998) 3-Amino-5-hydroxybenzoic acid in antibiotic biosynthesis. XI. Biological origins and semisynthesis of thionaphthomycins, and the structures of naphthomycins I and J. J Antibiot 51:845–851
14. Ikeda C, Hayashi Y, Itoh N, Seto H, Dairi T (2007) Functional analysis of eubacterial *ent*-copalyl diphosphate synthase and pimara-9(11),15-diene synthase with unique primary sequences. J Biochem 141:37–45
15. Ikeda H, Kotaki H, Omura S (1987) Genetic studies of avermectin biosynthesis in *Streptomyces avermitilis*. J Bacteriol 169:5615–5621
16. Ikeda H, Nonomita T, Usami M, Ohta T, Omura S (1999) Organization of the biosynthetic gene cluster for the polyketide anthelmintic macrolide avermectin in *Streptomyces avermitilis*. Proc Natl Acad Sci USA 96:9509–9514
17. Ikeda H, Ishikawa J, Hanamoto A, Shinose M, Kikuchi H, Shiba T, Sakaki Y, Hattori M, Omura S (2003) Complete genome sequence and comparative analysis of the industrial microorganism *Streptomyces avermitilis*. Nat Biotechnol 21:526–531
18. Jothivasan CK, Hamilton CJ (2008) Mycothiol: synthesis. Biosynthesis and biological functions of the major low molecular weight thiol in actinomyccetes. Nat Prod Rep 25:1091–1117
19. Ketterer B (1982) The role of nonenzymatic reactions of glutathione in xenobiotic metabolism. Drug Metab Rev 13:161–187
20. Komatsu M, Takano H, Hiratsuka T, Ishigaki Y, Shimada K, Beppu T, Ueda K (2006) Proteins encoded by the conservon of *Streptomyces coelicolor* A3(2) comprise a membrane-associated heterocomplex that resembles eukaryotic G protein-coupled regulatory system. Mol Microbiol 62:1534–1546
21. Komatsu M, Tsuda M, Omura S, Oikawa H, Ikeda H (2008) Identification and functional analysis of genes controlling biosynthesis of 2-methylisoborneol. Proc Natl Acad Sci USA 105:7422–7427
22. Komatsu M, Uchiyama T, Omura S, Cane DE, Ikeda H (2010) Genome-minimized *Streptomyces* host for the heterologous expression of secondary metabolism. Proc Natl Acad Sci USA 107:2646–2651
23. Komatsu M, Komatsu K, Koiwai H, Yamada Y, Kozone I, Izumikawa M, Hashimoto J, Takagi M, Omura S, Shin-ya K, Cane DE, Ikeda H (2013) Engineered *Streptomyces avermitilis* host for heterologous expression of biosynthetic gene cluster for secondary metabolites. ACS Synth Biol 2:384–396
24. Koyama N, Tokura Y, Takahashi Y, Tomoda H (2011) New cyslabdans B and C, potentiators of imipenem activity against methicillin-resistant *Staphylococcus aureus* produced by *Streptomyces* sp. K04-0144. Acta Pharm Sin B 1:236–239
25. Koyama N, Tokura Y, Münch D, Sahl HG, Schneider T, Shibagaki Y, Ikeda H, Tomoda H (2012) The nonantibiotic small molecule cyslabdan enhances the potency of beta-lactams against MRSA by inhibiting pentaglycine interpeptide bridge synthesis. PLoS ONE 7:e48981
26. Koyama T (1999) Molecular analysis of prenyl chain elongation enzymes. Biosci Biotechnol Biochem 63:1671–1676
27. McCaskill D, Croteau R (1997) Prospects for the bioengineering of isoprenoid biosynthesis. Adv Biochem Eng Bio/Technol 55:107–146
28. Newton GL, Av-Gay Y, Fahey RC (2000) *N*-Acetyl-1-D-myo-inosityl-2-amino-2-deoxy-α-D-glucopyranoside deacetylase (MshB) is a key enzyme in mycothiol biosynthesis. J Bacteriol 182:6958–6963
29. Newton GL, Fahey RC (2002) Mycothiol biochemistry. Arch Microbiol 178:388–394
30. Noma M, Suzuki F, Gamou K, Kawashima N (1982) Two labdane diterpenoids from *Nicotiana raimondii*. Phytochemistry 21:395–397
31. Ohtawa M, Hishinuma Y, Takagi E, Yamada T, Ito F, Uchida R, Kim Y-P, Omura S, Tomoda H, Nagamitsu T (2015) Structural revision and protecting group-free synthesis of cyslabdan (**in preparation**)
32. Omura S, Fujimoto T, Otoguro K, Matsuzaki K, Moriguchi R, Tanaka H, Sasaki Y (1991) Lactacystin, a novel microbial metabolite, induces neuritogenesis of neuroblastoma cells. J Antibiot 44:113–116
33. Rawat M, Uppal M, Newton G, Steffek M, Fahey RC, Av-Gay Y (2004) Targeted mutagenesis of the *Mycobacterium smegmatis mca* gene, encoding a mycothiol-dependent detoxification protein. J Bacteriol 186:6050–6058
34. Rynkiewicz MJ, Cane DE, Christianson DW (2001) Structure of trichodiene synthase from *Fusarium sporotrichioides* provides mechanistic inferences on the terpene cyclization cascade. Proc Natl Acad Sci USA 98:13543–13548
35. Seemann M, Zgai G, Kraker JW, Paschall CM, Christianson DW, Cane DE (2002) Pentalenene synthase. Analysis of active site residues by site-directed mutagenesis. J Am Chem Soc 124:7681–7689
36. Starks CM, Back K, Chappell J, Noel JP (1997) Structural basis for cyclic terpene biosynthesis by tobacco 5-*epi*-aristolochene synthase. Science 277:1815–1820
37. Takano H, Hashimoto K, Yamamoto Y, Beppu T, Ueda K (2001) Pleiotropic effect of a null mutation in the cvn1 conservon of *Streptomyces coelicolor* A3(2). Gene 477:12–18
38. Tetzlaff CN, You Z, Cane DE, Takamatsu S, Omura S, Ikeda H (2006) A gene cluster for biosynthesis of the sesqui-terpenoid antibiotic pentalenolactone in *Streptomyces avermitilis*. Biochemistry 45:6179–6186

39. Yamada Y, Cane DE, Ikeda H (2012) Diversity and analysis of bacterial terpene synthases. In: Hopwood DA (ed) Chapter seven, Natural product biosynthesis by microorganisms and plants, part A, methods in enzymology, vol 515. Academic Press, New York, pp 123–166
40. Yamada Y, Kuzuyama T, Komatsu M, Shin-ya K, Omura S, Cane DE, Ikeda H (2015) Terpene synthases are widely distributed in bacteria. Proc Natl Acad Sci USA 112:857–862
41. Yamada Y, Arima S, Nagamitsu T, Johmoto K, Uekusa H, Eguchi T, Shin-ya K, Cane DE, Ikeda H (2015) Novel terpenes generated by heterologous expression of bacterial terpene synthase genes in an engineered *Streptomyces* host. J Antibiot 68:385–394